Influence of Nongyrotropy in the Electron Beam-plasma Interaction

M. A. E. de Moraes*, Y. Omura† and M. V. Alves*

*INPE-LAP, PO. Box 515, 12245-970, S. J. Campos, SP
†Radio Science Center for Space & Atmosphere, Kyoto University, Japan

Abstract. Nongyrotropic particle species have been detected in most regions of geoplasma, the distant solar wind, and cometary environments. In this work we performed particle simulations of beam-plasma interaction in a one-dimensional system taken along the magnetic field. We introduced a nongyrotropy in the particle population of an electron beam drifting against the background plasma. We study possible electromagnetic emissions. In the nongyrotropic case, we found that the magnetic field energy became much larger than in the gyrotropic case, indicating a strong electromagnetic wave emission.

INTRODUCTION

Distribution functions in magnetoplasmas of the type $F(v_{\|}, v_{\perp})$, where velocities occur both parallel ($v_{\|}$) and perpendicular ($v_{\perp}$) to the bacgkground magnetic field ($\vec{B}_0$) are symmetric with respect to the magnetic field and are termed gyrotropic. When this symmetry is broken, the distribution becomes gyrophase dependent or nongyrotropic [1].

Nongyrotropic magnetoplasmas with a background field $\vec{B}_0 = B_0\hat{x}$ have at least one particle population whose unperturbed distribution function depends on the gyrophase angle $\varphi = \tan^{-1}(v_z/v_y)$ [2]. The effects of nongyrotropy on linear wave dispersion were first studied in the context of fusion plasmas [3, 4]. Several studies followed this pionnering researches. They showed that the introduction of gyrophase organization (bunching) can bring about coupling among the parallel eingenmodes, with the associated free energy enhancing previously existing (gyrotropic) instabilities or, in otherwise stable media, generating wave growth [2, 5, 6, 7].

Nongyrotropic particle populations are frequently encountered in space plasmas. Nongyrotropy has been observed in ion populations in the region at and just upstream of Earth's bow schok [8], several Earth radii upstream [9] in the ion foreschok and dowstream in the magnetosheath [10]. Measurements by the ISEE1 and 2 indicates de existence of nongyrotropic electrons in these same regions [11].

In this work we performed particle simulations of electron beam-plasma interaction in a one-dimensional system taken along the magnetic field. We introduced a nongyrotropy in the particle population of an electron beam drifting against the background plasma. We study possible electromagnetic emissions. In the nongyrotropic case, we found that the magnetic field energy became much larger than in the gyrotropic case, indicating a strong electromagnetic wave emission.

SIMULATION MODEL

We use a particle-in-cell code, KEMPO1 [12], that allows for spatial variations along x-direction. Since we are interested about parallel propagation, the wavevector of the modes is aligned with the x-direction, $\vec{k} = k\hat{x}$, with the ambient magnetic field defined by $\vec{B}_0 = B_0\hat{x}$.

For the proposed study the simulation code incorporates three species of charged particles: background electron and ions, and an electron beam with a given drift velocity. We assume the ion species to be of infinite mass, providing a neutralizing background. Both, beam and plasma electrons have maxwellian population. For gyrotropic and nongyrotropic cases the electrons of the beam are distributed with a pitch angle $\theta = 45^o$. For the nongirotropic case the electron beam presents also a drift velocity at the z-direction, v_{z0}, introduced at $t = 0$, which gives a gyrophase

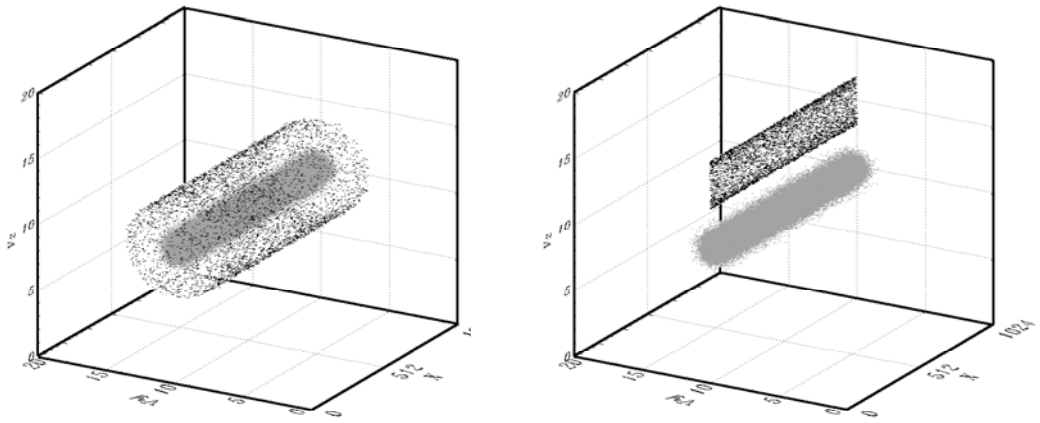

FIGURE 1. Particle velocity distribution, v_y and v_z as a function of propagation position x, at $t = 0$, for the gyrotropic case (rigth) and nongyrotropic case (left).

FIGURE 2. Time history of the electrostatic energy, $\propto E_x^2$, and kinetic energy, $(1/2)mv^2$; (a) and (b) for the gyrotropic case, and (c) and (d) for the nongyrotropic case.

angle $\varphi = 0^o$. Velocity distribution of the moving particles, gyrotropic and nongyrotropic cases, are shown in Figure 1, v_y and v_z as a function of position x, at $t = 0$. Boundary conditions are periodic and preexisting wave packets are not assumed, and all the waves grow self-consistently out of noise.

Electrostatic modes are investigated by observing the longitudinal wave electric fields ($\overrightarrow{E} \parallel \overrightarrow{k} \parallel \hat{x}$) whereas the electromagnetic modes by observing the wave field components (E_y, E_z), and (B_y, B_z).

RESULTS AND DISCUSSION

Simulation results presented in this section were obtained using the following computational parameters: electron plasma frequency, $\omega_p^2 = \omega_{pe}^2 + \omega_{pb}^2 = 1$; electron cyclotron frequency, $\Omega_e = 0.5$; electron thermal velocity, $v_{th} = 0.02c$; electron beam thermal velocity, $v_{bth} = 0.002c$; electron beam drift velocity $v_{bx0} = 0.1c$; grid spacing, $\Delta x = 0.1c/\omega_p$; number of grid points, 1024; number of superparticles, 4096000; time step, $0.005\omega_p^{-1}$; beam to plasma density ratio, $n_b/n_0 = 0.04$.

Figure (2 presents the time evolution of electrostatic and kinetic energy for the gyrotropic ((a) and (b)) and nongyrotropic case ((c) and (d)). At $t = 0$, the nongyrotropic case presents a higher kinetic energy due to the introduction of $v_{z0} \neq 0$. We can observe that until $t \simeq 50\omega_{pe}^{-1}$ both cases present similar behaviour, the corresponding decreasing of kinetic energy appearing as an increasing of electrostatic energy. For $t \simeq 100\omega_{pe}^{-1}$, the decreasing of kinetic energy does not show up as an increasing of electrostatic energy, for the nongyrotropic case (see Figure 2).

Concerning the electromagentic energy, we see that for the gyrotropic case there is no variation along the time, as shown in Figure 3(a), and (b). For the nongyrotropic case, we see an increasing of the electromagnetic energy as shown in Figure 3(d). The growing of electromagnetic energy starts at $t \simeq 80\omega_p^{-1}$reaching the first maximum at $t \simeq 100\omega_p^{-1}$, coincident with the point where the kinetic energy starts to decrease (see Figure 2).

The diagram $\omega \times k$ tells us the modes that are present in the system. We constructed the $\omega \times k$ diagram for the electromagnetic fields components (E_x, E_y, E_z, B_y,and B_z). We will show the $\omega \times k$ diagram for E_x, and E_z. Figure (4 shows the $\omega \times k$ diagram for E_x component (electrostatic mode) for the gyrotropic (top) and the nongytropic case (bottom). Grey scale is related to the intensity of the field component (in dB). For both cases we observe Langmuir waves, frequency close to 1, forward and backwrad propagating and also the beam mode forward propagating. Gyrotropic and nogyrotropic cases present very similar behaviour.

Figure (5) shows the $\omega \times k$ diagram for the E_z component (electromagnetic mode) for the gyrotropic (top) and the nongytropic case (bottom). For both cases we observe the RCP and LCP high frequency modes, forward and backward propagating. We also observe the whistler mode (RCP low frequency) in both cases, but for the nongyrotropic case

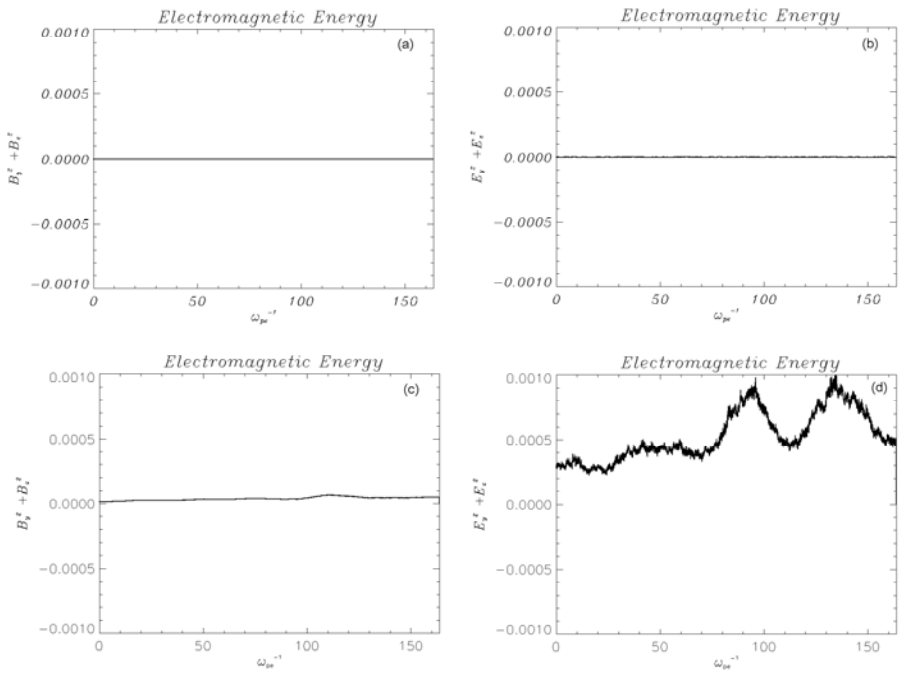

FIGURE 3. Time history of the electromagnetic energy, $\propto B_y^2 + B_z^2$ (a) and (c), and $\propto E_y^2 + E_z^2$, (b) and (d), for the gyrotropic case ((a) and (c)) and for the nongyrotropic case ((c) and (d).

FIGURE 4. $\omega \times k$ diagram for the electric field component, E_x, electrostatic, for the gyrotropic case (top) and for the nongyrotropic case (bottom). Grey scales are related to the amplitude of the component.

this mode emission is intensified. Scale color is related to the intensity of the field component (in dB). We also observe in the nongyrotropic case a localized emission (nonpropagating) and a second branch in the whistler mode backward propagating.

The behaviour of the system can also be illustrated by the phase space of the particles ($v_x \times x$). Figure 6 show the phase space for beam and plasma electrons for different times. At early times, up to $t = 90\omega_p^{-1}$, the behaviour of the systems, gyrotropic (left) and nongyrotropic (right), are similar to each other and also similar to an electrostatic electron beam-plasma interaction. For later times, the nongyrotropic case presents a cell formation in the phase space, indicating that electrons are trapped in their own potential. The last picture is shown for $t \simeq 160\omega_p^{-1}$.

CONCLUSIONS

In this work we performed particle simulations of electron beam-plasma interaction in a one-dimensional system taken along the magnetic field. We introduced a nongyrotropy in the particle population of an electron beam drifting against the background plasma. We compare the behaviour of two systems, gyrotropic and nongyrotropic. We observe that at early times, up to $t = 90\omega_p^{-1}$,both systems have similar behaviour. For times larger than $90\omega_p^{-1}$, there is an enhancement of the electromagnetic energy for the nongyrotropic case. An intensification of the emission of the whistler mode can be observed in the $\omega \times k$ diagram for the E_z component (see Figure 5). Phase space of the beam and the plasma electrons also shows the different behaviour for the late times for the gyrotropic and nongyrotropic cases.

FIGURE 5. $\omega \times k$ diagram for the electric field component, E_z, electromagnetic mode, for the gyrotropic case (top) and for the nongyrotropic case (bottom).

FIGURE 6. Phase space ($v_x \times x$) for the beam and plasma electrons for three different time steps, gyrotropic (top) and nongyrotropic (bottom) cases. At $t = 0$ both cases have the same phase space.

Different gyrophase angles and density beam to plasma ratios should be investigated in the near future.

ACKNOWLEDGMENTS

This work is supported by FAPESP-Fundação de Amparo à Pesquisa do Estado de São Paulo, Brazil

REFERENCES

1. U. Motschamann, H. Kafemann, and M. Scholer, Ann. Geophysicae, 15, 603, 1997
2. F. J. Romeiras, and A. L. Brinca, J. Geophys. Res.104, 12407, 1999
3. R. N. Sudan, Phys. of Plasmas, 8, 1915, 1965
4. O. Eldridge, Phys. of Plasmasn 13, 1791, 1970
5. A. L. Brinca, L. Borda de Água, and D. Winske, Geophys. Res. Let. 12(24), 2445, 1992
6. A. L. Brinca, L. Borda de Água, and D. Winske, J. Geophys. research, 98, 7549, 1993
7. A. L. Brinca, J. Atmospheric and Solar-Terrestrial Physics, 62, 701, 2000
8. J. T. Gosling, S. J. Bames, and C. T. Russel, J. Geophys. Res., 90, 270, 1985
9. C. Gurgiolo, G. K. Parks, B. H. Mauk, C. S. Lin, A. Anderson, R. P. Lin, and H. Rème, J. Geophys. Res., 86, 4415, 1981
10. N. Sckopke, G. Paschmann, A. L. brinca, C. W. Carlson, H. Lür, J. Geophys. res., 95, 6337, 1990
11. K. A. Anderson, R. P. Lin, C. Gurgiolo, G. K. Parks, D. W. Potter, S. Werden, and H. Rème, J. Geophys. Res., 90, 10809, 1985
12. Y. Omura, and H. Matsumoto, in: Computer Space Plasma Physics, ed. by H. Matsumoto and Y. Omura, Chap.2, 21-84, 1993